Rock physics modelling and inversion for saturation-pressure changes in time-lapse seismic studies

Xiaozheng Lang* and Dario Grana

Department of Geology and Geophysics, School of Energy Resources, University of Wyoming, Laramie, WY 82071, USA

ABSTRACT

Time-lapse seismic data are generally used to monitor the changes in dynamic reservoir properties such as fluid saturation and pore or effective pressure. Changes in saturation and pressure due to hydrocarbon production usually cause changes in the seismic velocities and as a consequence changes in seismic amplitudes and travel times. This work proposes a new rock physics model to describe the relation between saturation-pressure changes and seismic changes and a probabilistic workflow to quantify the changes in saturation and pressure from time-lapse seismic changes. In the first part of this work, we propose a new quadratic approximation of the rock physics model. The novelty of the proposed formulation is that the coefficients of the model parameters (i.e. the saturation-pressure changes) are functions of the porosity, initial saturation and initial pressure. The improvements in the results of the forward model are shown through some illustrative examples. In the second part of the work, we present a Bayesian inversion approach for saturation-pressure 4D inversion in which we adopt the new formulation of the rock physics approximation. The inversion results are validated using synthetic pseudo-logs and a 3D reservoir model for CO_2 sequestration.

Key words: Inversion, Monitoring, Reservoir geophysics, Rock physics, Time lapse.

INTRODUCTION

During reservoir production, time-lapse seismic data can be used to monitor reservoir changes by repeatedly acquiring 3D seismic data (Landrø 2001; Lumley 2001; Calvert 2005; Abriel 2008; Thore and Hubans 2012; Bjørlykke 2010; Lumley *et al.* 2015; Thore and Blanchard 2015; Maharramov, Biondi and Meadows 2016). This monitoring method has been successfully applied in different field cases to indirectly measure pressure and saturation changes in hydrocarbon reservoirs and carbon dioxide sequestration studies (Landrø *et al.* 2003; Arts *et al.* 2004; Vedanti and Sen 2009; Grude, Landrø and Osdal 2013; Blanchard and Delommot 2015). The estimation of saturation and

pressure changes from time-lapse seismic data requires the knowledge of the physical relation that links the dynamic changes to the seismic changes (Abriel 2008). The changes in elastic properties can be generally predicted through a rock physics model and the corresponding changes in the seismic response are predicted through a wave propagation model (Avseth, Mukerji and Mavko 2005; Mavko, Mukerji and Dvorkin 2009; Dvorkin, Gutierrez and Grana 2014).

The saturation effect on seismic velocities can be generally described by Gassmann's equation combined with the mass balance equation for density. In general, if water replaces hydrocarbon, the density of the saturated rock increases due to the higher density of water, the P-wave velocity increases due to the higher bulk modulus of water and the S-wave velocity decreases since the fluid shear modulus is 0 and the fluid only affects the density in the S-wave velocity expression. For the pressure effect on seismic velocities, a comprehensive

*E-mail: xlang@uwyo.edu

relation is still not available, but several empirical equations have been proposed (Eberhart-Phillips, Han and Zoback 1989; Hofmann *et al.* 2005; MacBeth 2004; Sayers 2006, among the others). In general, if effective pressure increases, the P-wave and S-wave velocity of the rock increase, whereas the density remains approximately the same. Such increase is more significant at low effective pressure than high effective pressure. Indeed, many models are based on exponential relations that tend to an asymptotical value for large pressure values. Assuming that the effective pressure is defined as the difference between the overburden pressure and the pore pressure, similar conclusions can be drawn for pore pressure changes. If the pore pressure increases, then the velocity generally decreases. Pore pressure affects the elastic properties of the fluid, as described by Batzle–Wang relations (Batzle and Wang 1992), but it is normally a secondary effect compared to the effect on the saturated rock. Differently from the saturation effect, the calibration of the pressure relations generally requires a set of laboratory measurements where the dry elastic moduli are measured at different effective pressure conditions (Han 1986). The above-introduced rock physics models allow computing the changes in elastic properties when the initial and final saturation-pressure conditions are known. The seismic response, in terms of reflectivity, as well as amplitude and travel-time, can be approximated using a convolutional model (Aki and Richards 1980; Stolt and Weglein 1985; Buland and Omre 2003). Many time-lapse inversion studies are performed in two steps (Buland and El Ouair 2006; Doyen 2007): first the changes in elastic properties are estimated from time-lapse seismic data; then, the changes in saturation and pressure are estimated from the changes in elastic properties estimated in the first step.

Landrø (2001) presents a rock physics model approximation that expresses changes in density using a linear approximation in the changes in saturation, and changes in velocities using an approximation that is linear in the saturation changes and quadratic in the pressure changes. By combining this approximation with Aki–Richards linear approximation of the seismic reflectivity coefficients, Landrø (2001) derives an approximation of the changes in the reflectivity coefficients as a polynomial function of the changes in saturation and pressure. The time-lapse inversion can be solved very efficiently using gradient-based methods. Successful applications have been proposed for hydrocarbon reservoirs (Landrø *et al.* 2003) as well as CO_2 sequestration studies (Grude *et al.* 2013). Other inversion methods such as stochastic optimization algorithms could be applied using the same forward model in Landrø (2001). An example of stochastic inversion approach

has been proposed in Veire, Borgos and Landrø (2006). Improvements to this formulation have been subsequently proposed by Meadows (2001), Trani *et al.* (2011) and Bhakta and Landrø (2014). Despite the common use of the formulation proposed by Landrø (2001), the method has some limitations. In particular, the approximation does not depend on porosity and does not depend on the initial saturation-pressure conditions but only on the property variations.

In the first part of this work, we propose a new formulation of the changes in reflectivity coefficients based on saturation-pressure changes. The formulation is inspired by the work of Landrø (2001), but in the proposed new formulation, the polynomial coefficients are functions of the reservoir rocks porosity, initial saturation and initial reservoir pressure. If a static model (before production) of porosity, saturation and pressure is available, the rock physics model with spatially varying coefficients can be applied in the time-lapse inversion workflow.

In the second part of this work, we use the new formulation in a Bayesian inversion scheme for the estimation of saturation-pressure changes from time-lapse seismic data. Because the proposed formulation is not linear, the Bayesian formulation presented in Buland and El Ouair (2006) cannot be applied; therefore, we adopt an ensemble-based method (Evensen 2009; Emerick and Reynolds 2013). The goal of introducing an inversion method is to show the advantages in using the proposed formulation of the porosity-dependent rock physics model compared to traditional methods that assume constant porosity and initial reservoir conditions.

The differences between the traditional models and the new formulation are shown through illustrative examples and synthetic pseudo-wells. An example of application in 3D is shown using a reservoir model for CO_2 sequestration.

METHODOLOGY

This section is divided into three parts: review of existing rock physics models for saturation-pressure changes; new formulation of the rock physics model for saturation-pressure changes; Bayesian time-lapse inversion method. The first two parts focus on the forward rock physics model with the goal of deriving a more accurate approximation for time-lapse studies for saturation-pressure prediction, whereas the last part focusses on the inversion with the goal of showing the effect of the model accuracy on the inversion results.

Literature review

Rock physics models aim to predict the elastic response of saturated porous rocks. Most of the available models, such as empirical relations, granular media models and inclusion models, are derived for reservoir conditions in which the rock and fluid parameters are known (Mavko *et al.* 2009). If the fluid volumes change, the elastic properties change as well. Such effect is generally described by Gassmann's equation. Similarly, if the effective pressure changes, the elastic properties change too. Several empirical equations have been proposed to describe the pressure effect such as Eberhart-Phillips and MacBeth models (Eberhart-Phillips *et al.* 1989; MacBeth 2004). The associated seismic response can be approximated using a convolutional model (Aki and Richards 1980).

Landrø (2001) derived a new model to calculate the changes in velocities, densities and reflection coefficients in different reservoir conditions as a function of changes in pressure and saturation. The model for velocity changes is a polynomial approximation and it is linear in the saturation changes and quadratic in the pressure changes; the model for density changes is linear in the saturation changes and assumes that such changes are not affected by changes in effective pressure or that these changes are negligible (a similar assumption was used and validated in Han 1986; Eberhart-Phillips *et al.* 1989); the model for the reflection coefficient changes combines the previous relations with Aki–Richards linear approximation of Zoeppritz equation. If we indicate P-wave velocity with α, S-wave velocity with β and density with ρ, then the model can be formulated in terms of relative changes of elastic properties (i.e. the absolute change of the property divided by the initial value of the property), as follows:

$$\frac{\Delta \alpha}{\alpha} = \frac{\alpha' - \alpha}{\alpha} = l_\alpha \Delta s + m_\alpha \Delta p^2 + n_\alpha \Delta p, \tag{1}$$

$$\frac{\Delta \beta}{\beta} = \frac{\beta' - \beta}{\beta} = l_\beta \Delta s + m_\beta \Delta p^2 + n_\beta \Delta p, \tag{2}$$

$$\frac{\Delta \rho}{\rho} = \frac{\rho' - \rho}{\rho} = l_\rho \Delta s, \tag{3}$$

where α', β' and ρ' represent P-wave velocity, S-wave velocity and density, respectively, for the monitor survey; $\Delta \alpha$, $\Delta \beta$ and $\Delta \rho$ represent the absolute change in P-wave velocity, S-wave velocity and density, respectively, between the monitor survey and the baseline survey; Δs and Δp represent the changes in water saturation and effective pressure, and l_α, l_β, l_ρ, m_α, m_β, n_α and n_β are constant empirical coefficients which can be estimated from laboratory measurements. By assuming $\frac{\bar{\beta}'}{\bar{\alpha}'} \approx \frac{\bar{\beta}}{\bar{\alpha}}$ as in Landrø (2001; where the symbol ⁻ represents the average value of the property at the interface between upper

and lower layer), the changes in the reflection coefficients can be then written as

$$\Delta r_{pp}(\theta) = \frac{1}{2}\left(l_\rho \Delta s + l_\alpha \Delta s + m_\alpha \Delta p^2 + n_\alpha \Delta p\right)$$
$$+ \frac{1}{2}\left(l_\alpha \Delta s + m_\alpha \Delta p^2 + n_\alpha \Delta p\right)\tan^2\theta$$
$$- 4\frac{\bar{\beta}^2}{\bar{\alpha}^2}\left(m_\beta \Delta p^2 + n_\beta \Delta p\right)\sin^2\theta. \tag{4}$$

Meadows (2001) modified Landrø's equation by using a quadratic approximation for changes in water saturation and effective pressure as

$$\frac{\Delta \alpha}{\alpha} = k_\alpha \Delta s^2 + l_\alpha \Delta s + m_\alpha \Delta p^2 + n_\alpha \Delta p, \tag{5}$$

$$\frac{\Delta \beta}{\beta} = k_\beta \Delta s^2 + l_\beta \Delta s + m_\beta \Delta p^2 + n_\beta \Delta p, \tag{6}$$

$$\frac{\Delta \rho}{\rho} = k_\rho \Delta s^2 + l_\rho \Delta s, \tag{7}$$

where k_α, k_β, k_ρ, l_α, l_β, l_ρ, m_α, m_β, n_α and n_β are empirical constant values. The expression for the changes in the reflection coefficients can be derived similar to equation (4).

The assumption behind Landrø's equations (equations (1)–(3)) and Meadows' equations (equations (5)–(7)) is that the regression coefficients are same everywhere in the entire reservoir.

Proposed formulation

The main limitation of Landrø's equations (equations (1)–(3)) and Meadows' equations (equations (5)–(7)) is that they do not account for the porosity of the rock, nor the initial saturation and pressure, but are only functions of the absolute change. The use of constant empirical values simplifies the calculations in the inversion approach but it introduces a limitation because if the equations are calibrated using, for example high-porosity rock samples, and the equation is applied to low-porosity rock samples, it might lead to biased predictions of the elastic and seismic response variations. Similarly, the equations should also depend on the initial saturation and pressure values and not only on the absolute changes. Changes in effective pressure at low effective pressure conditions (e.g. from 5 to 10 MPa) produce a more significant variation in elastic properties than changes at high effective pressure (e.g. from 35 to 40 MPa): indeed, many of the physical models proposed for the pressure effect assume exponential trends. In mixtures of gas and water, a small amount of gas (such as 5% of gas) in a brine-saturated rock causes a large drop in P-wave velocity, whereas an increase in gas from 5% to 100% causes
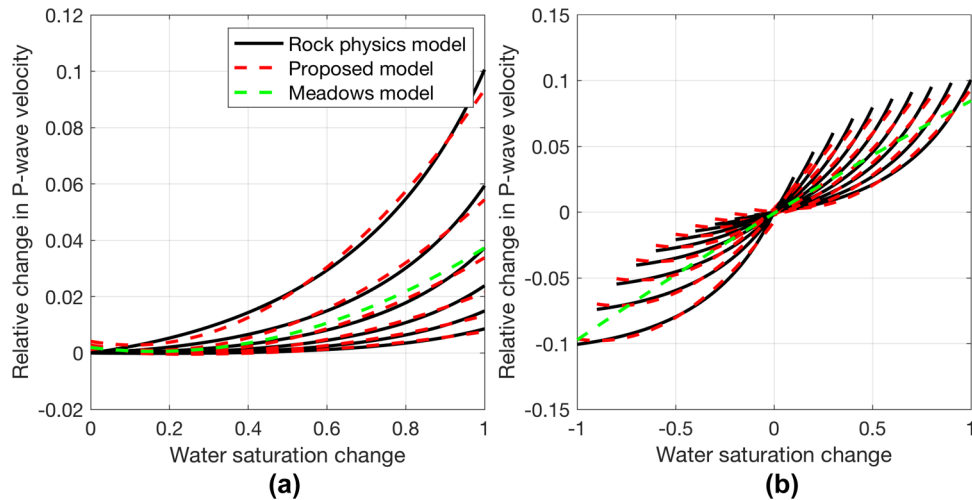
Figure 1 Rock physics relations between relative change in P-wave velocity and water saturation change and comparison of full rock physics model (black lines), proposed approximation (red lines) and Meadows' equation (green lines). (a) Water saturation is 0 in the baseline survey and increases up to 1 in the monitor survey; each line represents different porosity values varying, from top to bottom, from 0.1 to 0.35 respectively. (b) Porosity is constant and equal to 0.35; each line represents different initial water saturation values varying from 0 to 1.

a small change in P-wave velocity: indeed, the bulk modulus of a mixture of gas and water is often computed using Reuss harmonic relation (Mavko *et al.* 2009).

In this work, we propose a quadratic approximation for the relative changes of elastic properties in which the approximation coefficients are functions of the reservoir porosity, initial water saturation and initial effective pressure. To facilitate the use of the proposed model in time-lapse seismic inversion, we express the approximation in the logarithm of

the ratio of the properties of the monitor seismic survey and the properties of the baseline seismic survey in order to combine the proposed formulation with the approximation of the reflection coefficients proposed by Stolt and Weglein (1985) and adopted by Buland and El Ouair (2006).

By combining equations (5)–(7) with Aki–Richards approximation, we can derive the expression for the change in reflectivity equivalent to equation (4) proposed in Landrø (2001). The proposed formulation is based on Meadows'
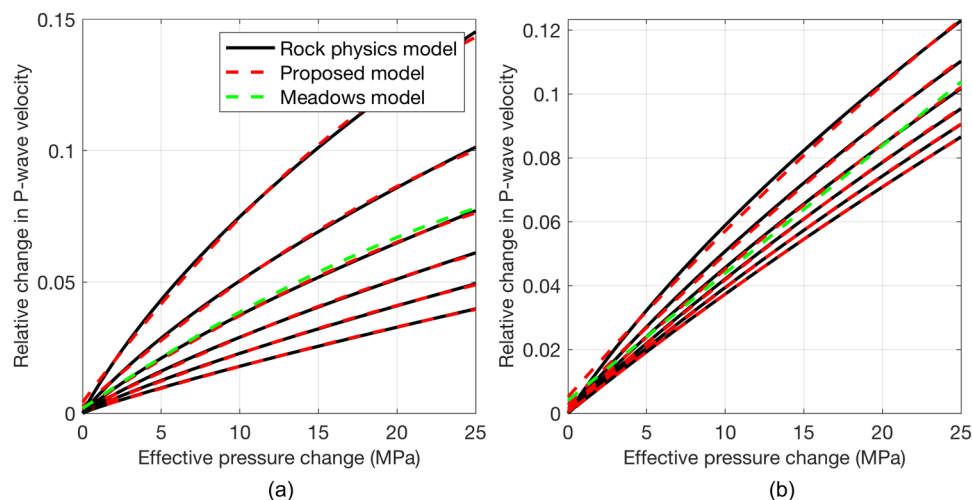

Figure 2 Rock physics relations between relative change in P-wave velocity and effective pressure change, and numerical comparison of full rock physics model (black lines), proposed model (red lines) and Meadows' approximation (green lines). (a) Effective pressure is 5 MPa in baseline survey and increases up to 30MPa in the monitor survey; each line represents different porosity values varying, from top to bottom, from 0.1 to 0.35 respectively. (b) Porosity is constant and equal to 0.35; each line represents different initial effective pressure varying from 10to 35 MPa.
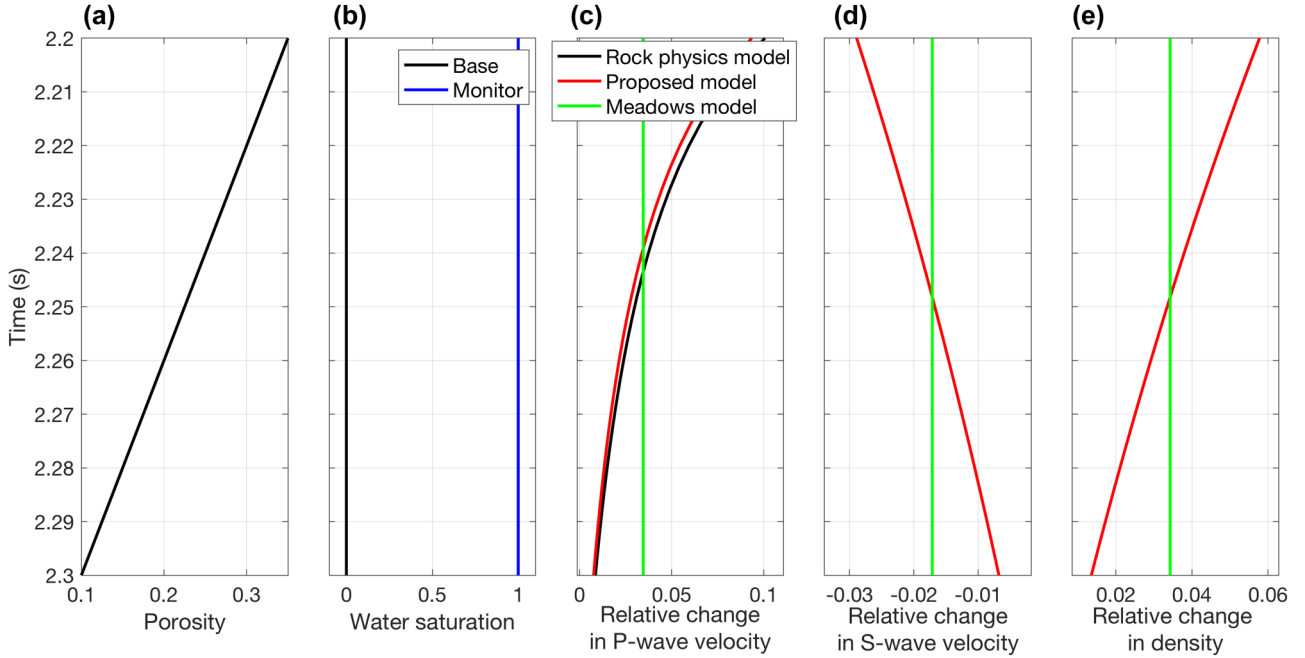
Figure 3 Illustrative example to study the porosity effect on the relative change of elastic properties assuming a constant water saturation change and constant effective pressure. (a) Porosity, (b) initial and final saturation, (c) relative change of P-wave velocity, (d) relative change of S-wave velocity and (e) relative change of density (full rock physics model in black, proposed model in red and Meadows' equation in green).

relation but the coefficients vary spatially and are functions of the initial conditions:

$$\ln \frac{\alpha'(t)}{\alpha(t)} = k_\alpha(\phi, s)\,\Delta s^2 + l_\alpha(\phi, s)\,\Delta s + m_\alpha(\phi, p)\,\Delta p^2$$
$$+ n_\alpha(\phi, p)\,\Delta p, \tag{8}$$

$$\ln \frac{\beta'(t)}{\beta(t)} = k_\beta(\phi, s)\,\Delta s^2 + l_\beta(\phi, s)\,\Delta s + m_\beta(\phi, p)\,\Delta p^2$$
$$+ n_\beta(\phi, p)\,\Delta p, \tag{9}$$

$$\ln \frac{\rho'(t)}{\rho(t)} = k_\rho(\phi, s)\,\Delta s^2 + l_\rho(\phi, s)\,\Delta s, \tag{10}$$

where for simplicity we indicated the travel-time variable t but not the spatial variables (x, y), and where α', β' and ρ' represent P-wave velocity, S-wave velocity and density, respectively, for the monitor survey; and α, β and ρ represent P-wave velocity, S-wave velocity and density, respectively, for the base survey. Instead of using constant values for the coefficients, the parameters k_α, k_β, k_ρ, l_α, l_β, l_ρ, m_α, m_β, n_α, n_β are empirical functions of porosity ϕ, initial water saturation s and initial effective pressure p, computed by fitting quadratic

regressions to experimental data. For example, the coefficients for equation (8) are computed as follows:

$$k_\alpha(\phi, s) = a_2(s)\,\phi^2 + a_1(s)\,\phi + a_0, \quad a_i = a_{i,1}s + a_{i,0}, \tag{11}$$

$$l_\alpha(\phi, s) = b_2(s)\,\phi^2 + b_1(s)\,\phi + b_0, \quad b_i = b_{i,1}s + b_{i,0}, \tag{12}$$

$$m_\alpha(\phi, s) = c_2(p)\,\phi^2 + c_1(p)\,\phi + c_0, \; c_i = c_{i,1}p + c_{i,0}, \tag{13}$$

$$n_\alpha(\phi, s) = d_2(p)\,\phi^2 + d_1(p)\,\phi + d_0, \; d_i = d_{i,1}p + d_{i,0}, \tag{14}$$

for $i = 0, 1, 2$. Similar expressions can be derived for the coefficients in equations (9) and (10). The polynomial coefficients in equations (11)–(14) must be calibrated from core data or well logs.

To show the advantage of using the proposed formulation compared to the original formulation by Meadows (2001), we built a synthetic dataset using a rock physics model based on the stiff-sand model (Dvorkin *et al.* 2014), Gassmann's equation and an empirical relation for pressure. The comparison is done using the relative changes in P-wave velocity. The dataset includes rock samples with porosity ranging from 0.10 to 0.35 with different initial saturation and pressure and the P-wave velocity is computed in different saturation and pressure conditions. Figures 1 and 2 show the comparison between the actual rock physics model and the approximated models.
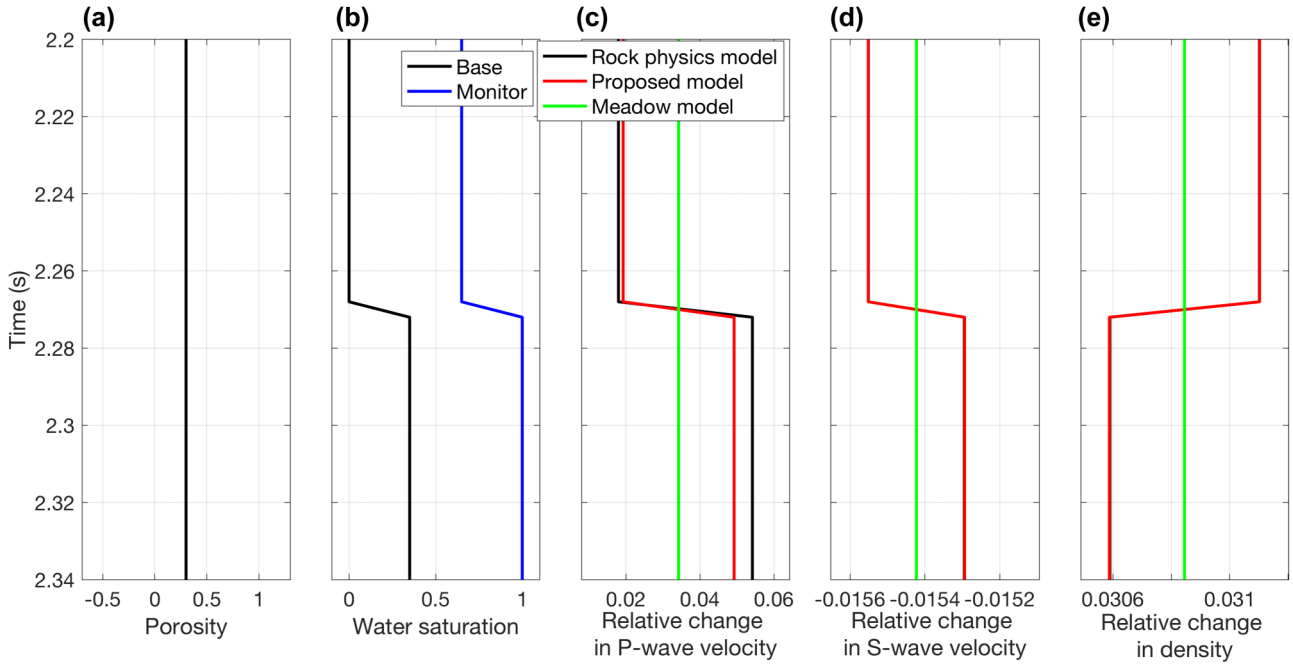
Figure 4 Illustrative example to study the effect of initial water saturation on the relative change of elastic properties assuming constant effective pressure. Legend and colours as in Fig. 3.

In Fig. 1(a), we compute the P-wave velocity assuming that water saturation is 0 everywhere in the baseline survey and changes from a minimum of 0 in the baseline survey to a maximum of 1 in the monitor survey, due to the water injection (pressure is assumed to be constant). Therefore, the change in water saturation varies between 0 (no change in saturation between baseline and monitor survey) and 1 (the entire oil volume present in the baseline survey is fully replaced by water in the monitor survey). Intermediate values between 0 and 1 represent partial saturations during injection. Each sample (black lines) represents a different rock with porosity equal to 0.1, 0.15, 0.20, 0.25, 0.30 and
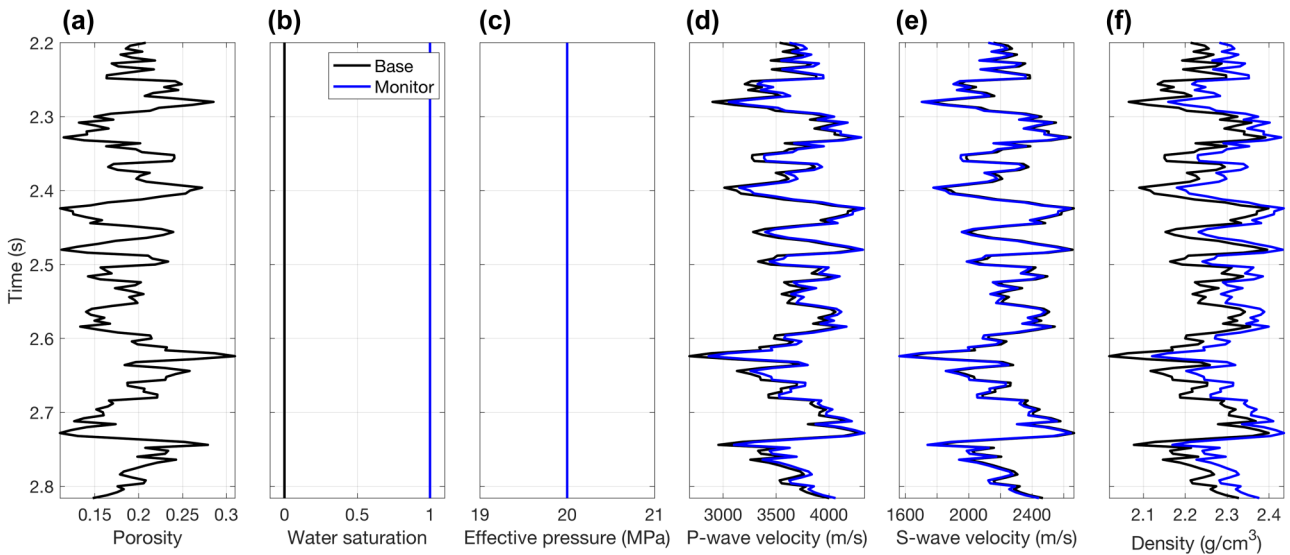

Figure 5 Example with synthetic well logs, from left to right. (a) Porosity, (b) water saturation, (c) effective pressure, (d) P-wave velocity, (e) S-wave velocity and (f) density. Data for the baseline survey are in black, data for the monitor survey are in blue.
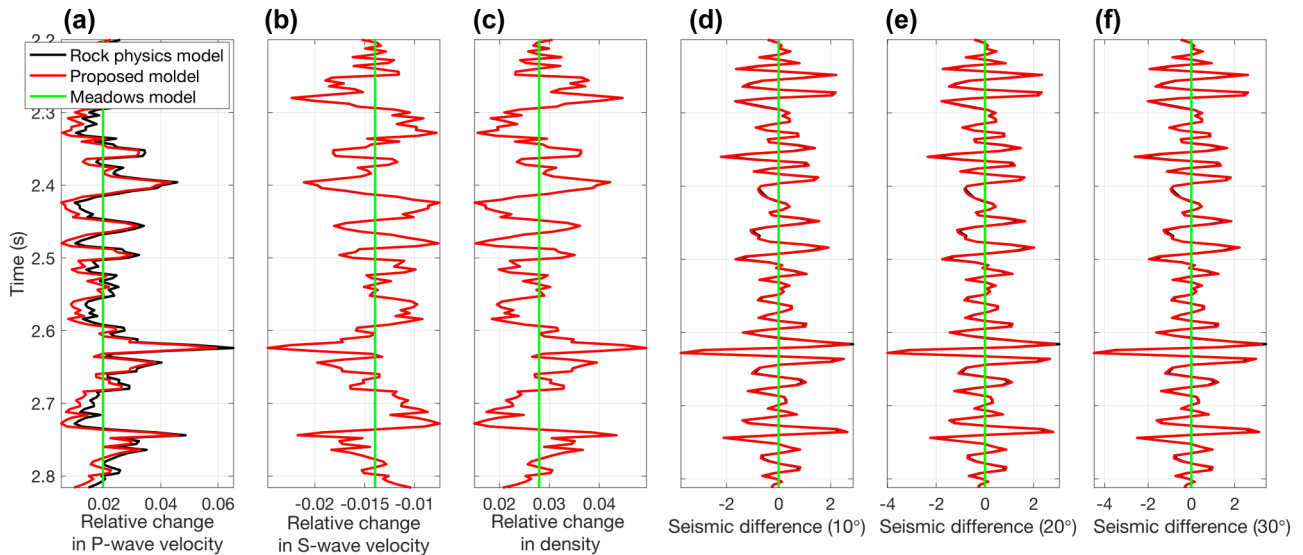
Figure 6 Numerical comparison of the forward models: full rock physics model (black lines), proposed model (red lines) and Meadows' equation (green lines). From left to right: (a) relative change in P-wave velocity, (b) relative change in S-wave velocity, (c) relative change in density, (d) seismic amplitude differences for the near angle (10°), (e) seismic amplitude differences for the mid angle (20°) and (f) seismic amplitude differences for the far angle (30°).

0.35. The results show that the change in elastic properties due to the change in water saturation is different for rocks with different porosities. Because Meadows' equation (green
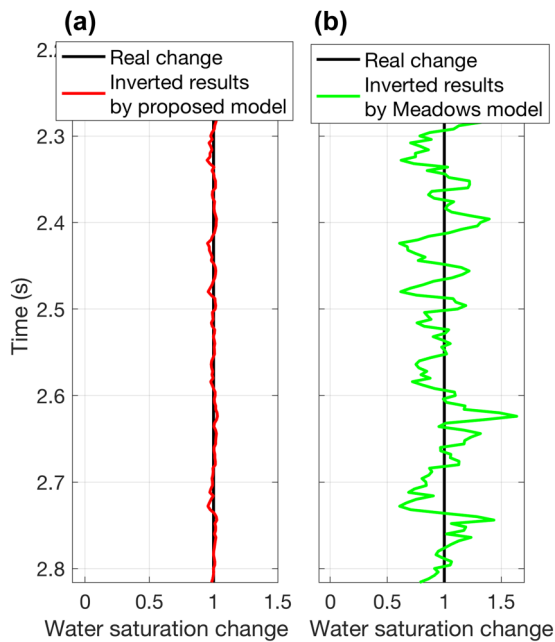

Figure 7 Comparison of the inverted results obtained with the proposed formulation (a) and Meadows' equation (b). The actual changes are shown in black, the inverted results using the proposed formulation in red and the inverted results using Meadows' formulation in green.

line) does not account for porosity, the approximation can be computed only for an average value (0.225 in this example); however, the proposed formulation (red lines) matches the synthetic dataset with good accuracy.

Figure 1(b) describes the effect of the initial water saturation on the relative change of P-wave velocity: in this example, porosity is a fixed value equal to 0.35 and different initial water saturation values, varying from 0 to 1, are assumed. The synthetic dataset was computed using the full rock physics model. Water saturation changes from the two end-point scenarios: 100% of oil and 100% of water. If water saturation in the baseline survey is 1, then water saturation can decrease down to 0; therefore, the change of water saturation varies between 0 (no fluid change, meaning that the reservoir is fully saturated by water at the time of the monitor survey) and −1 (oil has fully replaced water). If water saturation in the baseline survey is 0.1, then water saturation can increase up to 1 because of water injection and production of oil (e.g. in hydrocarbon reservoirs); therefore, the change in water saturation varies between 0 (no change) and 0.9 (fully saturated by water, since the initial water saturation was 0.1). Each sample (black lines) has a different initial water saturation, therefore the range of the water saturation change is different for each sample: for example, if the initial water saturation is 0.1, the maximum change in water saturation is 0.9; if the initial water saturation is 0.7, the maximum change in water saturation is 0.3. The trends computed using the full rock physics model
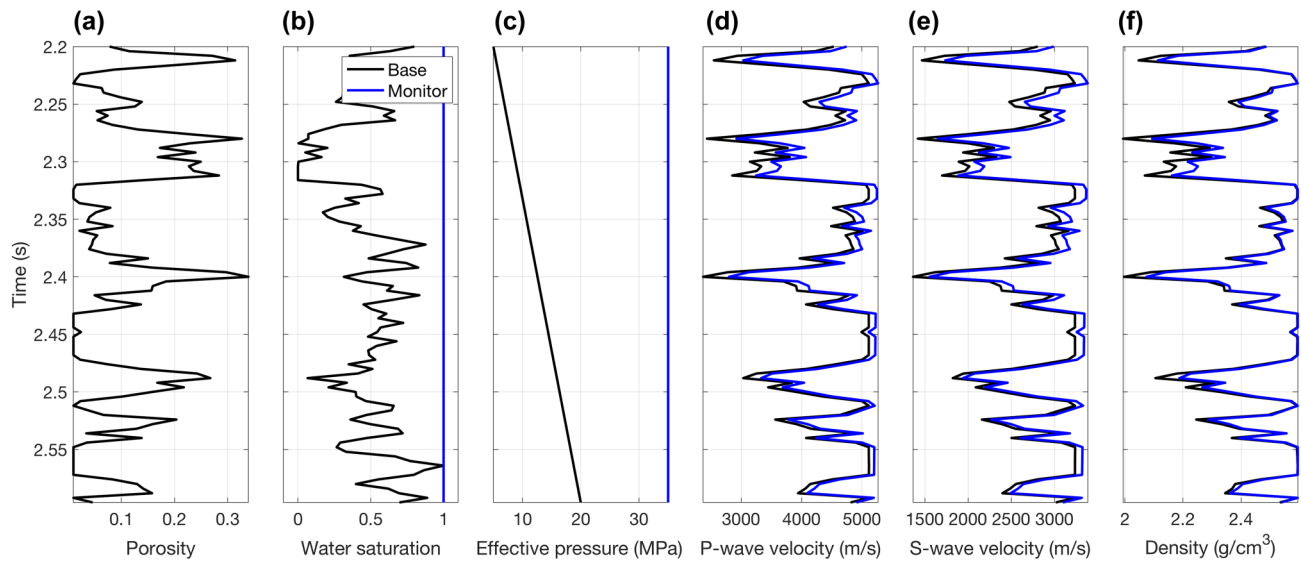
Figure 8 Example with synthetic well logs. Legend and colours as in Fig. 5.

can be approximated by the proposed approximation (red lines) that accounts for the effect of the initial water saturation, whereas Meadows' equation (green line) only provides an average value.

Figure 2(a) shows the relation between relative changes in P-wave velocity and the effective pressure change, assuming that the initial effective pressure in the baseline survey is 5 MPa and it changes from a minimum of 0 to a maximum of 25 MPa. Each sample (black lines) represents a different rock with porosity equal to 0.1, 0.15, 0.20, 0.25, 0.30 and 0.35. The approximated model accounting for the porosity effect (red lines) fits the full rock physics model (black lines). Figure 2(b) describes the effect of the initial effective pressure on the relative change of P-wave velocity: in this example, porosity is a fixed value equal to 0.35 and different initial effective pressure values, varying from 10 to 35 MPa, are assumed. For simplicity, in this example, we assume that effective pressure can only increase and the maximum values is 60 MPa (for an initial pressure of 35 MPa), but similar results can be obtained for different initial and final pressure conditions. The results show that the initial effective pressure affects the relative change in P-wave velocity with respect to pressure change. Each sample (black lines) has a different initial effective pressure, from 10 to 35 MPa, and the change in pressure varies between 0 to 25 MPa; therefore, for an initial pressure of 10 MPa, the maximum value is 35 MPa, whereas for an initial pressure of 35 MPa, the maximum value is 60 MPa. Meadows' equation (green line) only provides an average value, whereas the proposed approximation (red lines)

that accounts for the effect of the initial pressure conditions correctly approximate the measurements simulated using the full rock physics model.

Bayesian inversion

The model proposed in equations (8)–(14) can be integrated in many inversion schemes proposed in the geophysics literature. It could be used with non-linear least square methods (Dadashpour, Landrø and Kleppe 2008), such as gradient and conjugate gradient algorithms, as well as probabilistic inversion methods, such as Bayesian inversion (Aster, Borchers and Thurber 2011; Tarantola 2005). In our approach, we propose a Bayesian inversion method.

Similar to Buland and El Ouair (2006), we work with the differences of seismic amplitudes between the baseline seismic survey and the monitor seismic survey. We use partial stacked seismic data, and assume that data have been preliminary processed according to a standard seismic processing workflow and each angle stack have been corrected for time shift to align horizons between base and monitor surveys (using, e.g. a warping method, as in Hale 2009; Ayeni 2011; Pazetti *et al.* 2016). The goal of the inversion is to estimate the changes in saturation and pressure from the seismic amplitudes difference of time-lapse seismic data (either between the monitor and baseline surveys or between two repeated monitor surveys). Similar to Buland and El Ouair (2006), the forward model can be expressed in the following form:

$$\Delta \mathbf{d} = \mathbf{f}(\Delta \mathbf{q}) + \boldsymbol{\varepsilon} = \mathbf{f}(\mathbf{g}(\Delta \mathbf{m})) + \boldsymbol{\varepsilon}, \tag{15}$$
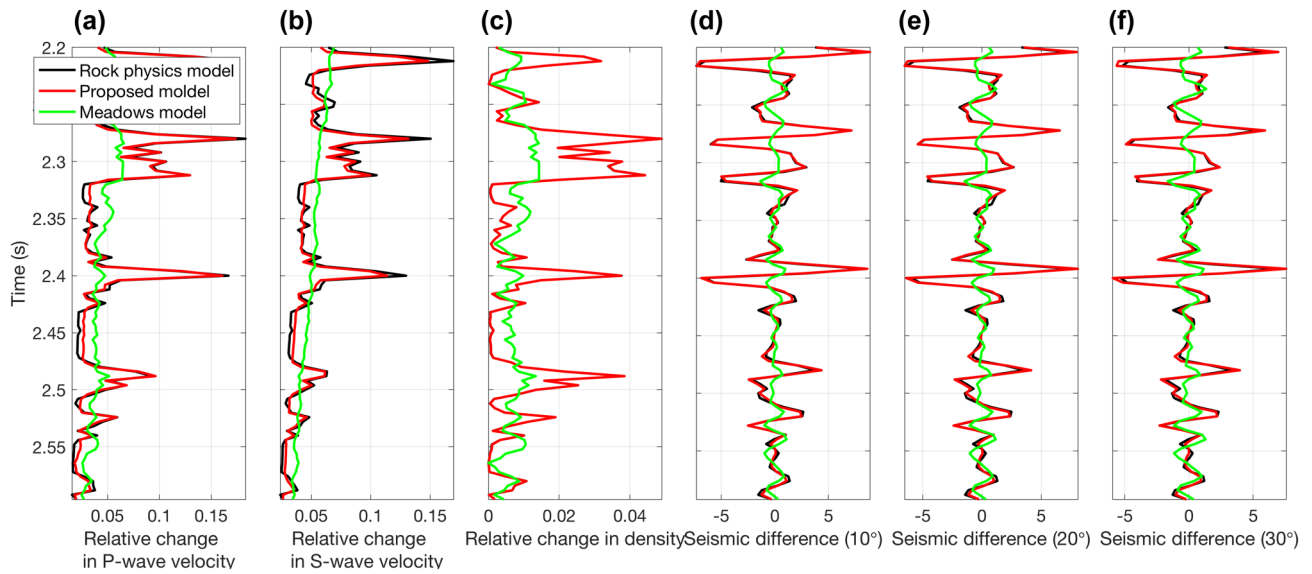
Figure 9 Numerical comparison of the forward models: full rock physics model. Legend and colours as in Fig. 6.

where Δd represents the seismic amplitude differences, Δq represents the changes in elastic parameters, Δm represents the changes in saturation and pressure, ε is the error in the seismic measurements related to the noise in the data, f is the seismic forward model and g is the rock physics model. In this work, we focus on pressure and saturation and we assume that all the other reservoir parameters, such as porosity, do

not change during time. We also assume that systematic errors in the time-lapse seismic data have been corrected in the processing; therefore, the error term ε is assumed to be distributed according to a Gaussian function with zero mean and known standard deviation, as in Buland and El Ouair (2006).

If we adopt a convolutional model for the forward seismic model for a given survey (e.g. the baseline survey), the seismic
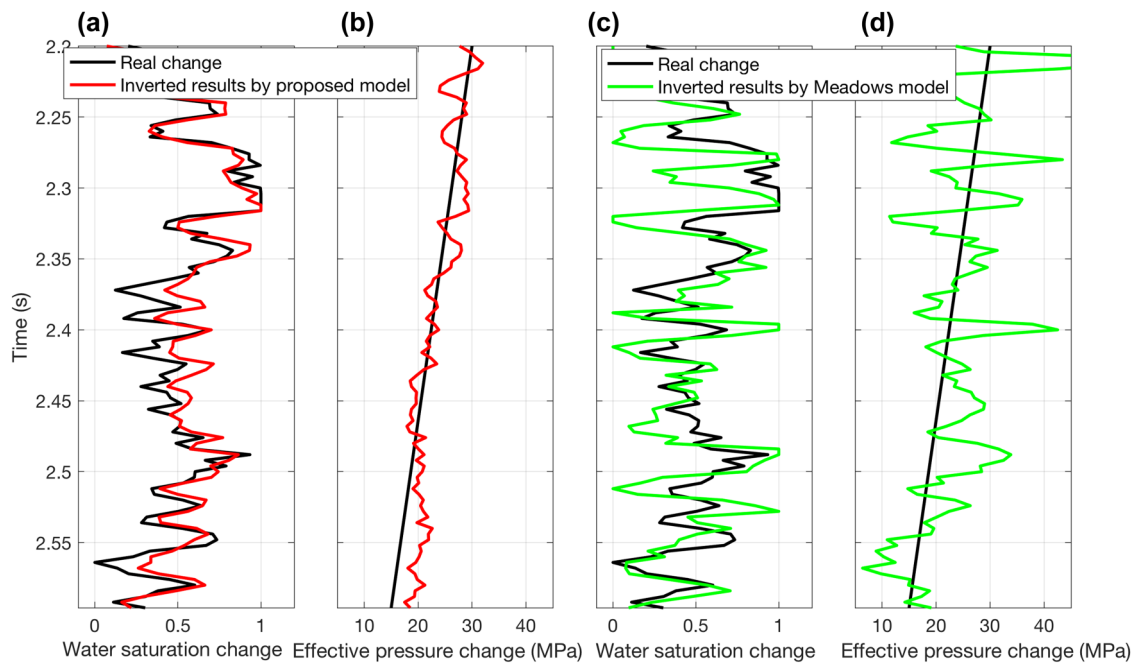

Figure 10 Comparison of the inverted results obtained with the proposed formulation (a) and Meadows' equation (b). Legend and colours as in Fig. 7.

data d of the survey can be computed as a linear function of the reflectivity using a convolution with a known wavelet as

$$\mathbf{d} = \mathbf{W}\mathbf{r}_{pp} + \boldsymbol{\varepsilon}, \tag{16}$$

where $\mathbf{W}$ is the matrix associated with the seismic wavelet and r_{pp} is the weak contrast PP reflectivity computed by Aki–Richards equation (Aki and Richards 1980; Stolt and Weglein 1985; Buland and Omre 2003):

$$r_{pp}(t, \theta) = \frac{1}{2}\left(1 + \tan^2\theta\right)\frac{\partial}{\partial t}\ln\alpha(t) - 4\frac{\bar{\beta}^2}{\bar{\alpha}^2}\sin^2\theta\frac{\partial}{\partial t}\ln\beta(t)$$
$$+ \frac{1}{2}\left(1 - 4\frac{\bar{\beta}^2}{\bar{\alpha}^2}\sin^2\theta\right)\frac{\partial}{\partial t}\ln\rho(t), \tag{17}$$

where θ is the incident angle.

The same model can be used to predict the seismic data d' for any repeated monitor seismic survey, measured at a different time than the baseline survey. Because the model is linear, the same convolutional model can be also applied to seismic data difference, if data are preliminary corrected for time shifts (as in Buland and EI Ouair 2006; Grana and Mukerji 2015). If we indicate the seismic amplitude differences (after time warping) with $\Delta d = d' - d$ and we indicate the change in reflectivity with Δr_{pp}, then the time-lapse forward model can be written as

$$\Delta\mathbf{d} = \mathbf{W}\Delta\mathbf{r}_{pp} + \boldsymbol{\varepsilon}, \tag{18}$$

where the change of reflectivity Δr_{pp} at a given travel-time sample t:

$$\Delta r_{pp}(t, \theta) = \frac{1}{2}\left(1 + \tan^2\theta\right)\frac{\partial}{\partial t}\ln\frac{\alpha'(t)}{\alpha(t)} - 4\frac{\bar{\beta}^2}{\bar{\alpha}^2}\sin^2\theta\frac{\partial}{\partial t}\ln\frac{\beta'(t)}{\beta(t)}$$
$$+ \frac{1}{2}\left(1 - 4\frac{\bar{\beta}^2}{\bar{\alpha}^2}\sin^2\theta\right)\frac{\partial}{\partial t}\ln\frac{\rho'(t)}{\rho(t)}, \tag{19}$$

assuming $\frac{\bar{\beta}'}{\bar{\alpha}'} \approx \frac{\bar{\beta}}{\bar{\alpha}}$, as in Landrø (2001).

The rock physics model g in equation (15) can be approximated using the proposed approximation in equations (8)–(14). By combining equations (8)–(14) with Aki–Richards approximation in equation (19), we obtain the expression for the change in reflectivity as

$$\Delta r_{pp}(t, \theta)$$
$$= \frac{1}{2}\left(1 + \tan^2\theta\right)\frac{\partial}{\partial t}\ln\left(k_\alpha(\phi, s)\Delta s^2\right)$$
$$+ l_\alpha(\phi, s)\Delta s + m_\alpha(\phi, p)\Delta p^2 + n_\alpha(\phi, p)\Delta p)$$
$$- 4\frac{\bar{\beta}^2}{\bar{\alpha}^2}\sin^2\theta\frac{\partial}{\partial t}\ln\left(k_\beta(\phi, s)\Delta s^2 + l_\beta(\phi, s)\Delta s\right)$$

$$+ m_\beta(\phi, p)\Delta p^2 + n_\beta(\phi, p)\Delta p)$$
$$+ \frac{1}{2}\left(1 - 4\frac{\bar{\beta}^2}{\bar{\alpha}^2}\sin^2\theta\right)\frac{\partial}{\partial t}\left(k_\rho(\phi, s)\Delta s^2 + l_\rho(\phi, s)\Delta s\right). \tag{20}$$

The resulting model is used as the forward model for the inverse problem in equation (15). Because the inverse problem is non-linear in the model parameters Δs and Δp, the analytical solution proposed in Buland and El Ouair (2006) is not available and a numerical approach must be adopted. In our application, the inversion scheme used to solve the inverse problem is the ensemble smoother with multiple data assimilation (Emerick and Reynolds 2013), where an ensemble of several realizations of saturation and pressure changes is iteratively updated conditioned by the measured time-lapse seismic amplitudes. Each single Bayesian updating step can be expressed in the form

$$\Delta\mathbf{m}_k^u = \Delta\mathbf{m}_k^p + \mathbf{C}_{\Delta m \Delta d}^p\left(\mathbf{C}_{\Delta d \Delta d}^p + \mathbf{C}_\varepsilon\right)^{-1}\left(\widetilde{\Delta d}_k - \Delta d_k^p\right), \tag{21}$$
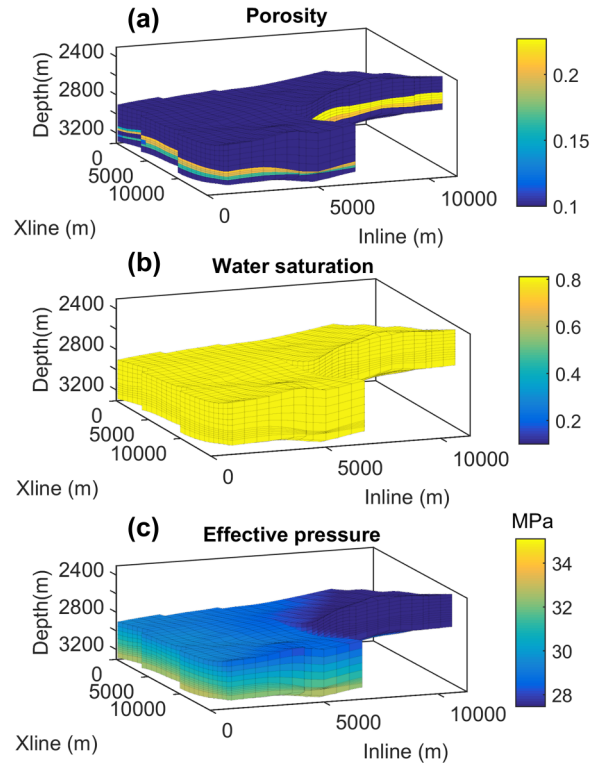

Figure 11 Reservoir properties of the Johansen model before CO_2 injection (depth of the baseline survey): (a) porosity, (b) water saturation and (c) effective pressure.
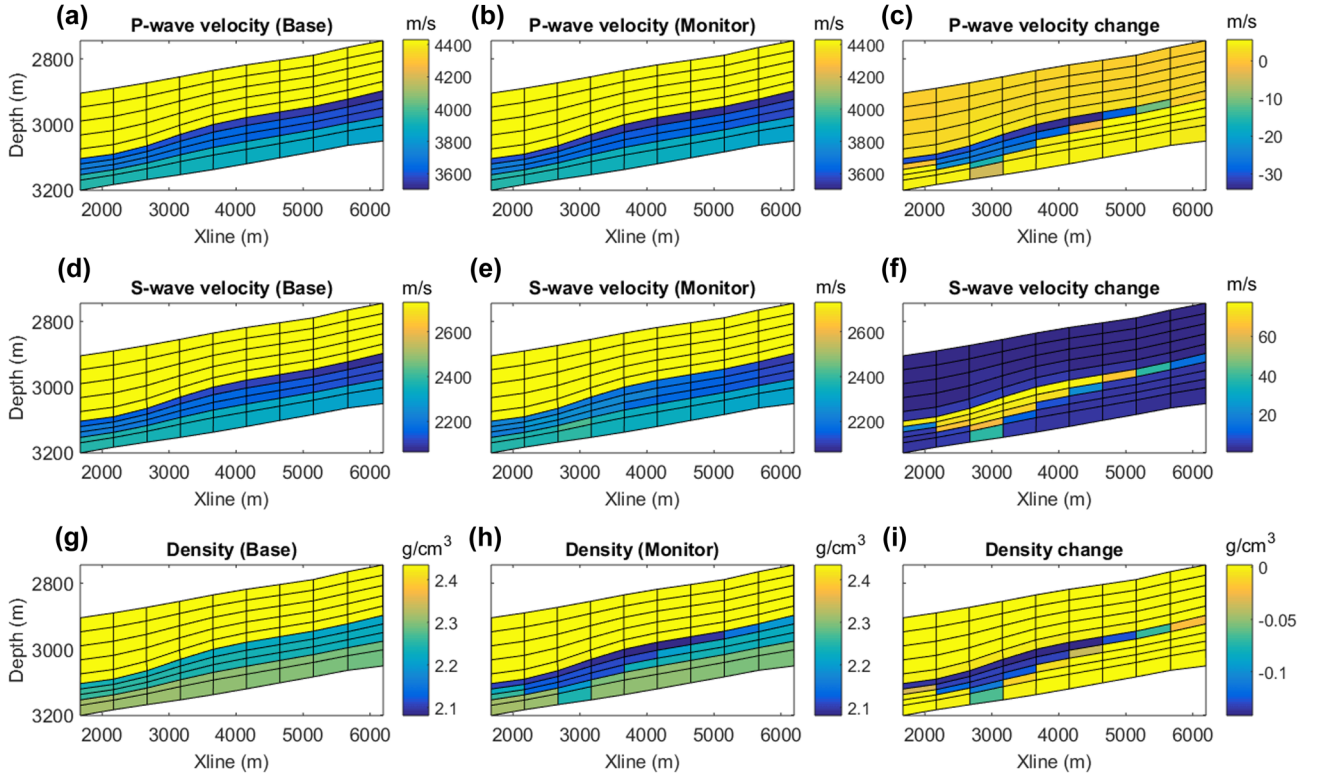
Figure 12 Two-dimensional section of elastic properties computed using the full rock physics model in depth domain: (a) P-wave velocity (baseline), (b) P-wave velocity (monitor), (c) absolute P-wave velocity change between baseline and monitor, (d) S-wave velocity (baseline) (e) S-wave velocity (monitor), (f) absolute S-wave velocity change, (g) density (baseline), (h) density (monitor) and (i) absolute density change.

where $k = 1, \ldots N$ represent the ensemble models, the model parameters are $\Delta m = [\Delta s, \quad \Delta p]^T$, the superscript p indicates the model at the previous iteration and the superscript u indicates the updated model, $C_{\Delta m \Delta d}$ represents the cross-covariance between the model parameters and the data, $C_{\Delta d \Delta d}$ represents the covariance of the data, C_{ε} is the co-variance of the error term, $\widetilde{\Delta d}_k$ is a stochastic perturbation of the measured data (measured seismic differences) and Δd_k is the predicted data (predicted amplitude differences). The Bayesian updating steps is iterated multiple times until convergence (Emerick and Reynolds 2013).

APPLICATIONS

Illustrative examples

To validate the proposed approximation of the forward model (equations (8)–(14)), we build a set of illustrative examples to show the limitations of the current approximations and the improvement provided by the proposed formulation. In these examples, we change the reservoir conditions (porosity and initial reservoir conditions) to study its effect on the elastic response. We show the different reservoir conditions using pseudo-logs, but we point out that the sequence of samples is not supposed to mimic realistic logs but idealized situations in order to analyse the relation between reservoir conditions and geophysical response. In Fig. 3, we study the effect of porosity on the relative change of elastic properties assuming a constant water saturation change and constant effective pressure. In particular, we assume that porosity varies between 0.35 and 0.1, and that the reservoir at the time of the baseline survey (black line) is fully saturated with oil whereas at the time of the monitor survey (blue line) is fully saturated with water. The effective pressure is assumed to be 20 MPa in both surveys. In this example, we compare the actual data simulated using the full rock physics model (black lines), the approximated model using the proposed formulation (red lines) and Meadows' model (green lines). Because Meadows' equation does not account for porosity, the relative change in elastic properties is constant; however, the proposed formulation correctly approximates the full rock physics model for different porosity values.
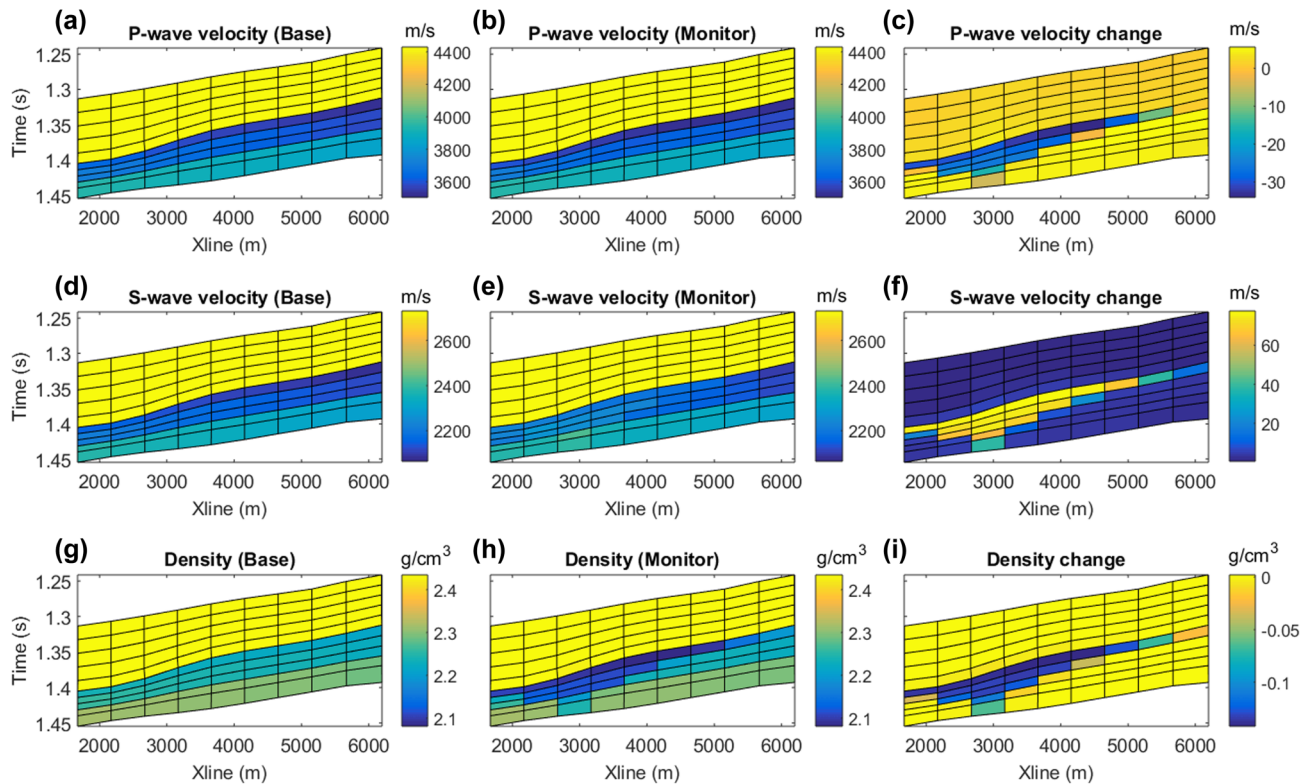
Figure 13 Two-dimensional section of elastic properties computed using the full rock physics model in time domain. Legend and colours as in Figure 12.

In Fig. 4, we study the effect of the initial water saturation assuming constant effective pressure. Indeed, the velocity relative change is not only function of the change in water saturation but also of the initial water saturation value. We assume that porosity is constant and equal to 0.3 and that effective pressure is constant and equal to 20 MPa. The initial water saturation is equal to 0 in the upper part (fully oil saturated) and 0.35 in the lower part (partially oil saturated). The water saturation change is constant and equal to 0.65; however due to the different initial water saturation, the water saturation for the monitor survey is equal to 0.65 in the upper part (0.35 of residual oil), and 1 in the lower part (fully water saturated). Because Meadows' equation (green line) is only based on the absolute change of water saturation, the relative change in elastic properties is constant; however, the proposed formulation (red lines) approximates the full rock physics model (black lines) for both saturation conditions.

Similar conclusions can be drawn by changing both porosity and initial saturation at the same time and for effective pressure changes in rock with different porosity

and/or different initial effective pressure. Other rock physics models can be used (Avseth *et al.* 2005; Avseth and Skjei 2011; Duffaut, Avseth and Landrø 2011; Avseth, Skjei and Skålnes 2013) such as the modified grain contact model (Saul, Lumley and Shragge 2013; Saul and Lumley 2015) or the patchy cement model (Avseth and Skjei 2011; Avseth, Skjei and Mavko 2016).

Synthetic examples

To validate the methodology, we created synthetic well logs to mimic potential pre- and post-production scenario. In the first scenario (Fig. 5), we created a pseudo-log of porosity using a geostatistical algorithm, assuming a Gaussian distribution with mean 0.2 and standard deviation 0.05 and using an exponential variogram model to ensure the spatial continuity. The water saturation is assumed to be 0 in the entire interval (fully oil saturated) at the time of the baseline survey and 1 in the entire interval (fully water saturated) at the time of the monitor survey. Effective pressure is assumed to be constant and equal to 20 MPa. The elastic properties, that is, P-wave velocity,
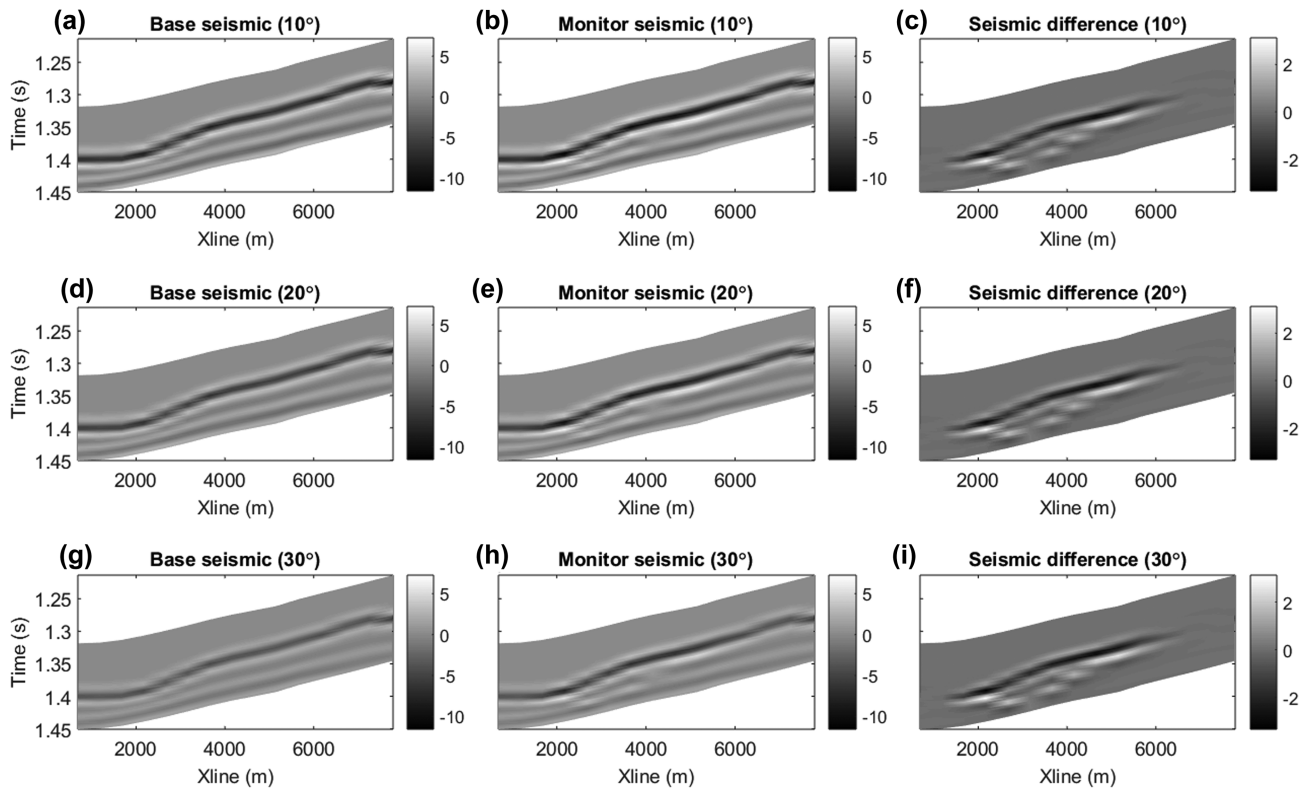
Figure 14 Synthetic time-lapse seismic data: (a) near angle (baseline), (b) near angle (monitor), (c) seismic amplitude differences for the near angle after warping, (d) mid-angle (baseline), (e) mid-angle (monitor), (f) seismic amplitude differences for the mid-angle, (g) far angle (baseline); (h) far angle (monitor) and (i) seismic amplitude differences for the far angle.

S-wave velocity and density, are computed using the stiff-sand model, Gassmann's equation and the density equation; the simulated data are shown in Fig. 5: the simulated data corresponding to the baseline survey are shown in black and the data for the monitor survey in blue. The corresponding relative changes in elastic properties and seismic data are shown in Fig. 6. The proposed approximated model matches the predicted changes; however, Meadows' equation predicts a constant value since the model does not depend on porosity and the water saturation is constant. The inverted results are shown in Fig. 7: the inverted results derived from the proposed model can correctly predict the water saturation change, whereas the inverted results from Meadows' equation mismatch the change in water saturation. Indeed, the errors in the prediction of water saturation correlate with the porosity log.

The second scenario (Fig. 8) represents a partially saturated reservoir with variable porosity and different effective pressure values ranging from 5 to 20 MPa at different depths. The initial water saturation was generated using a geostatistical algorithm assuming a Gaussian distribution with mean

0.5 and standard deviation 0.2 and using an exponential variogram. We assume that water injection took place in the well and that at the time of the monitor survey the reservoir is fully saturated by water and the pressure is constant and equal to 35 MPa in the entire interval. The relative changes of elastic properties and the corresponding seismic response are shown in Fig. 9. The results of the inversion are shown in Fig. 10. The forward and inverse models obtained using the proposed formulation allow obtaining a better result compared to Meadows' equation.

Field example

We finally apply the method to a synthetic seismic dataset generated from a reservoir model of the Johansen field located in Norway (Eigestad *et al.* 2009). The Johansen formation is a potential CO_2 storage site. The geo-cellular model including the reservoir and the sealing layers are made by 10 layers. Figure 11 shows porosity, water saturation and effective pressure for the pre-injection static model. The model includes over-cap layers of shale at the top, and a mid-to-high porosity
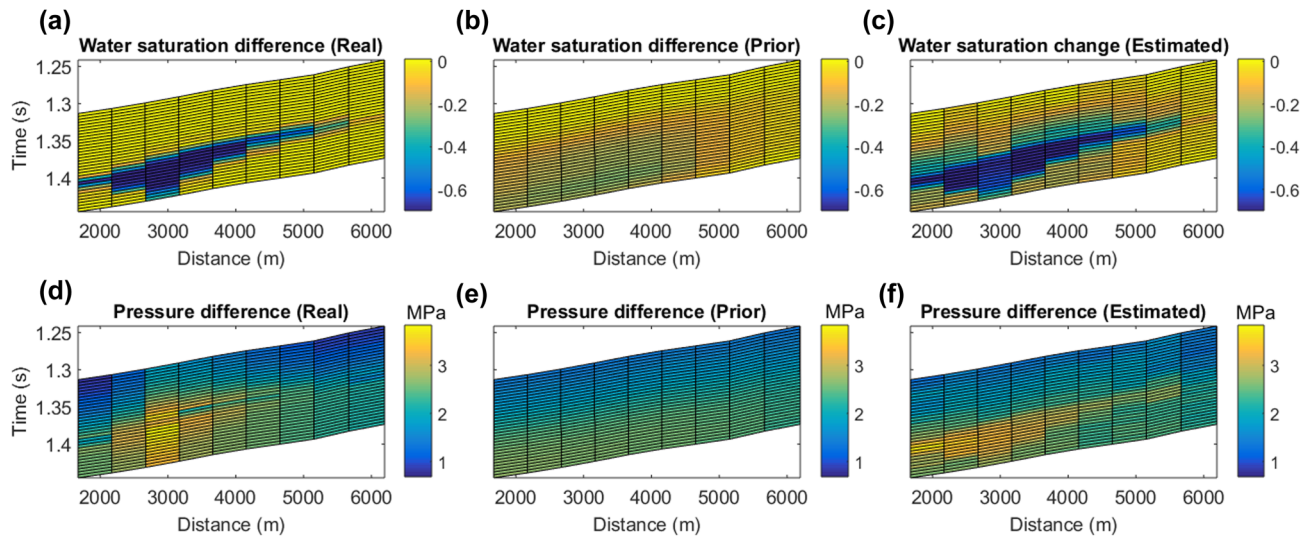
Figure 15 Comparison between the actual saturation-pressure changes and the estimated results. Top plots show water saturation and bottom plots show effective pressure: (a) actual water saturation change, (b) prior water saturation change, (c) predicted water saturation change, (d) actual effective pressure change, (e) prior effective pressure change and (f) predicted effective pressure change.

sandstone layer. We created a synthetic dataset by simulating CO_2 injection for 10 years using the Matlab Reservoir Simulation Toolbox for fluid flow simulation, and we computed a baseline survey (year 1) and a monitor survey (year 10). The synthetic dataset was computed using a convolutional model and a time-shift correction was applied to the monitor survey. The synthetic model is shown along a 2D section through the well location: the elastic properties computed using the full rock physics in depth domain are shown in Fig. 12, the elastic properties in time domain (sampling rate of 4 milliseconds) are shown in Fig. 13, and the seismic data are shown in Fig. 14. The $N = 100$ initial models of saturation and pressure in the ensemble were generated using geostatistical simulations (Doyen 2007); the average of the simulations is non-informative and assumes almost constant changes in the reservoir. The inversion results data are obtained using the approximated model proposed in the 'Methodology' section and the Bayesian inversion method based on the ensemble smoother algorithm. The inverted results are computed as the average of the 100 updated models of saturation and pressure in the ensemble. The results are shown in time domain in Fig. 15 and satisfactorily match the data.

DISCUSSION

This work presents an improvement of the approximated model to compute elastic and seismic changes (in terms of relative change of P-wave velocity, S-wave velocity, density

and reflectivity) due to changes in saturation and pressure. For reservoirs with unknown initial conditions, an average value of porosity can be assumed; in this scenario, the proposed approximation is equivalent to Meadow's equation, but for spatially variable reservoir conditions (i.e. different values in different locations of the reservoir) the proposed model is more accurate than linear and quadratic approximations proposed in the literature. The presented model can be used in time-lapse seismic inversion studies where the solution (i.e. the saturation-pressure changes) is computed directly from the changes in seismic amplitudes, as in Landrø (2001); however, the improved accuracy of the proposed model allows reducing the propagation of the errors due to the approximation of the forward physical operator to the solution of the inverse problem. In our work, we presented a quadratic approximation consistent with Meadows' equation, but theoretically a larger order polynomial could be used. The estimation of the coefficients of the quadratic expansion can be obtained by solving a non-linear least square problem to fit the values of well log data and core samples. Generally, the estimation of the coefficients for the water saturation change is easier than for pressure, since the model can be fitted using well logs before and after Gassmann's fluid substitution, whereas the pressure effect requires a set of laboratory measurements with velocities measured at different effective pressure conditions. The so-obtained model can be used for time-lapse seismic inversion in any inverse theory algorithm. In our work, we chose a probabilistic approach similar to Buland and El Ouair (2006).

However, the proposed formulation is quadratic; therefore, the analytical solution of the Bayesian inverse problem is not available. The main limitation of the proposed inversion is that it requires a pre-processing of the data to correct the monitor survey(s) for time shift. Time-shift information is very valuable for 4D seismic studies and its integration in the inversion workflow would improve the model predictions and reduce the prediction uncertainty; however, it is beyond the scope of this work. Furthermore, in this work, we assumed that porosity is variable in space, but constant in time; additional work to include the compaction effect is needed and could be developed using the formulations based on the dilation factor proposed by Røste, Stovas and Landrø (2006), Carcione *et al.* (2007) and Landrø (2015).

The proposed formulation and its utilization in Bayesian inversion allow improving the reservoir characterization as well as the ability to use time-lapse seismic data to monitor reservoir changes of dynamic properties including pressure and saturation. The implementation of the proposed method is beneficial not only for reservoir monitoring studies using time-lapse seismic but also for history matching problems (Oliver, Reynolds and Liu 2008). The integration of seismic data in history matching studies is challenging due to the large amount of data as well as the low resolution and low signal-to-noise ratio of the data; however, the application of the proposed methodology allows identifying the location of the fluid front as well as reservoir compartments with high and low effective pressure. Generally, seismic history matching problems include production data and elastic properties inverted from time-lapse seismic data (Huang, Meister and Workman 1997; Gosselin *et al.* 2003; Dong and Oliver 2005; Oliver and Chen 2011); however, the results of the proposed method allow directly integrating pressure and saturation in the seismic history matching workflow, which would allow solving the seismic history matching problem by adopting a parameterization (saturation and pressure) consistent with the fluid flow simulation.

CONCLUSIONS

We presented a methodology for the estimation and inversion of elastic and seismic property changes due to the changes in water saturation and effective pressure. The proposed model approximated the physics that describes how the elastic and seismic response of a sequence of porous rocks is affected by variations of water content and pressure conditions. The proposed formulation depends on the porosity of the rock, initial water saturation and initial effective pressure, and

provides an improvement compared to traditional approximations applied in time-lapse studies such as Landrø and Meadows' equations. The so-obtained formulation allows computing the change in reflectivity between two seismic surveys directly from the changes in water saturation and pressure and can be integrated in time-lapse seismic inversion studies through any inverse theory algorithm. In our work, we propose a Bayesian non-linear inversion algorithm based on the ensemble smoother multi-data assimilation to estimate the saturation-pressure changes given the difference in seismic amplitudes between two seismic surveys, after the preliminary warping process for the correction of the time shift. The validation through illustrative examples, synthetic well logs and a 3D reservoir model for CO_2 sequestration shows the improvement of the proposed forward model compared to traditional approximations and the inversion problem results.

REFERENCES

Abriel W. 2008. *Reservoir Geophysics: Applications*. Society of Exploration Geophysicists.

Aki K. and Richards P. 1980. *Quantitative Seismology*. W.H. Freeman.

Arts R., Eiken O., Chadwick A., Zweigel P., van der Meer L. and Zinszner B. 2004. Monitoring of CO_2 injected at Sleipner using time-lapse seismic data. *Energy* **29**, 1383–1392.

Aster C., Borchers B. and Thurber C. 2011. *Parameter Estimation and Inverse Problems*. Elsevier.

Avseth P., Mukerji T. and Mavko G. 2005. *Quantitative Seismic Interpretation*. Cambridge University Press.

Avseth P. and Skjei N. 2011. Rock physics modeling of static and dynamic reservoir properties – a heuristic approach for cemented sandstone reservoirs. *The Leading Edge* **30**, 90–96.

Avseth P., Skjei N. and Mavko G. 2016. Rock-physics modeling of stress sensitivity and 4D time shifts in patchy cemented sandstones – application to the Visund Field, North Sea. *The Leading Edge* **35**, 868–878.

Avseth P., Skjei N. and Skålnes Å. 2013. Rock physics modelling of 4D time-shifts and time-shift derivatives using well log data – a North Sea demonstration. *Geophysical Prospecting* **61**, 380–390.

Ayeni G. 2011. *Time-lapse seismic imaging by linearized joint inversion*. Ph.D. thesis, Stanford University.

Batzle M. and Wang Z. 1992. Seismic properties of pore fluids. *Geophysics* **57**, 1396–1408.

Bhakta T. and Landrø M. 2014. Estimation of pressure-saturation changes for unconsolidated reservoir rocks with high V_P/V_S ratio. *Geophysics* **79**, M35–M54.

Bjørlykke K. 2010. Petroleum geoscience: From sedimentary environments to rock physics. Springer Science & Business Media.

Blanchard D. and Delommot P. 2015. An example of the measurement and practical applications of time-lapse seismic attenuation. *Geophysics* **79**, WA25–WA34.

Buland A. and El Ouair Y. 2006. Bayesian time-lapse inversion. *Geophysics* **71**, R43–R48.

Buland A. and Omre H. 2003. Bayesian linearized AVO inversion. *Geophysics* **68**, 185–198.

Calvert R. 2005. *Insights and Methods for 4D Reservoir Monitoring and Characterization*. SEG and European Association of Geoscientists and Engineers.

Carcione J., Landrø M., Gangi A. and Cavallini F. 2007. Determining the dilation factor in 4D monitoring of compacting reservoirs by rock-physics models. *Geophysical Prospecting* **55**, 793–804.

Dadashpour M., Landrø M. and Kleppe J. 2008. Nonlinear inversion for estimating reservoir parameters from time-lapse seismic data. *Journal of Geophysical Engineering* **5**, 54–66.

Dong Y. and Oliver D. 2005. Quantitative use of 4D seismic data for reservoir description. *SPE Journal* **10**, 91–99.

Doyen P. 2007. *Seismic Reservoir Characterization*. EAGE.

Duffaut K., Avseth P. and Landrø M. 2011. Stress and fluid sensitivity in two North Sea oil fields – comparing rock physics models with seismic observations. *The Leading Edge* **30**, 98–102.

Dvorkin J., Gutierrez M. and Grana D. 2014. *Seismic Reflections of Rock Properties*. Cambridge University Press.

Eberhart-Phillips D., Han D.H. and Zoback M.D. 1989. Empirical relationships among seismic velocity, effective pressure, porosity, and clay content in sandstone. *Geophysics* **51**, 82–89.

Eigestad T., Dahle K., Hellevang B., Riis F., Johansen T. and Øian E. 2009. Geological modeling and simulation of CO_2 injection in the Johansen formation. *Computational Geosciences* **13**, 435.

Emerick A. and Reynolds A. 2013. Ensemble smoother with multiple data assimilation. *Computers & Geosciences* **55**, 3–15.

Evensen G. 2009. *Data Assimilation. The Ensemble Kalman filter*. Springer.

Gosselin O., Aanonsen S., Aavatsmark I., Cominelli A., Gonard R., Kolasinski M., *et al.* 2003. History matching using time-lapse seismic (HUTS). *Proceedings of the SPE Annual Technical Conference and Exhibition*, Denver, CO.

Grana D. and Mukerji T. 2015. Bayesian inversion of time-lapse seismic data for the estimation of static reservoir properties and dynamic property changes. *Geophysical Prospecting* **63**, 637–655.

Grude S., Landrø M. and Osdal B. 2013. Time-lapse pressure–saturation discrimination for CO_2 storage at the Snøhvit field. *International Journal of Greenhouse Gas Control* **19**, 369–378.

Hale D. 2009. A method for estimating apparent displacement vectors from time-lapse seismic images. *Geophysics* **74**, V99–V107.

Han D. 1986. Effects of porosity and clay content on acoustic properties of sandstones and unconsolidated sediments. Ph.D. thesis, Stanford University.

Hofmann R., Xu X., Batzle M., Prasad M., Furre A.-K. and Pillitteri A. 2005. Effective pressure or what is the effect of pressure?. *The Leading Edge* **24**, 1256–1260.

Huang X., Meister L. and Workman R. 1997. Reservoir characterization by integration of time-lapse seismic and production data. *Proceedings of the SPE Annual Technical Conference and Exhibition*, San Antonio, TX.

Landrø M. 2001. Discrimination between pressure and fluid saturation changes from time-lapse seismic data. *Geophysics* **66**, 836–844.

Landrø M. 2015. Chapter 19: 4D seismic, in Bjørlykke, K., Petroleum Geoscience, From Sedimentary Environments to Rock Physics: Springer.

Landrø M., Veire H., Duffaut K. and Najjar N. 2003. Discrimination between pressure and fluid saturation changes from marine multi-component time-lapse seismic data. *Geophysics* **68**, 1592–1599.

Lumley D. 2001. Time-lapse seismic reservoir monitoring. *Geophysics* **66**, 50–53.

Lumley D., Landrø M., Vasconcelos I., Eisner L., Hatchell P., Li Y., *et al.* 2015. Advances in time-lapse geophysics – introduction. *Geophysics* **80**, WAi–WAii.

MacBeth C. 2004. A classification for the pressure-sensitivity properties of a sandstone rock frame. *Geophysics* **69**, 497–510.

Maharramov M., Biondi B. and Meadows M. 2016. Time-lapse inverse theory with applications. *Geophysics* **81**, R485–R501.

Mavko G., Mukerji T. and Dvorkin J. 2009. *The Rock Physics Handbook*. Cambridge University Press.

Meadows M. 2001. Enhancements to Landrø's method for separating time-lapse pressure and saturation changes. 71th annual international meeting. SEG, Expanded Abstracts, 1652–1655.

Oliver D. and Chen Y. 2011. Recent progress on reservoir history matching, a review. *Computational Geosciences* **15**, 185–221.

Oliver S., Reynolds A. and Liu N. 2008. *Inverse Theory for Petroleum Reservoir Characterization and History Matching*. Cambridge University Press.

Pazetti B., Donno D., Davolio A., Grana D. and Schiozer D., 2016. The impact of time-shift estimation and correction on two 4D attributes-amplitude difference and velocity change. EAGE, Expanded Abstract.

Røste T., Stovas A. and Landrø M. 2006. Estimation of layer thickness and velocity changes using 4D prestack seismic data. *Geophysics* **71**, S219–S234.

Saul M. and Lumley D. 2015. The combined effects of pressure and cementation on 4D seismic data. *Geophysics* **80**, WA135–WA148.

Saul M., Lumley D. and Shragge J. 2013. Modeling the pressure sensitivity of uncemented sediments using a modified grain contact theory: Incorporating grain relaxation and porosity effects. *Geophysics* **78**, D327–D338.

Sayers C. 2006. Sensitivity of time-lapse seismic to reservoir stress path. *Geophysical Prospecting* **54**, 369–380.

Stolt R. and Weglein A. 1985. Migration and inversion of seismic data. *Geophysics* **50**, 2458–2472.

Tarantola A. 2005. *Inverse Problem Theory*. SIAM.

Thore P. and Blanchard T. 2015. 4D propagated layer-based inversion. *Geophysics* **80**, R15–R29.

Thore P. and Hubans C. 2012. 4D seismic-to-well tying, a key step towards 4D inversion. *Geophysics* **77**, R227–R238.

Trani M., Arts R., Leeuwenburgh O. and Brouwer J. 2011. Estimation of changes in saturation and pressure from 4D seismic and AVO time shift analysis. *Geophysics* **76**, C1–C17.

Vedanti N. and Sen M. 2009. Seismic inversion tracks in situ combustion: a case study from Balol oil field, India. *Geophysics* **74**, B103–B112.

Veire H., Borgos H. and Landrø M. 2006. Stochastic inversion of pressure and saturation changes from time-lapse AVO data. *Geophysics* **71**, C81–C92.